Chapter 11

# Organo-Soluble Semi-Alicyclic Polyimides Derived from Substituted-Tetralin Dianhydrides and Aromatic Diamines: Synthesis, Characterization and Potential Applications as Alignment Layer for TFT-LCDs

Jin-gang Liu, Yuan-zheng Guo, Hai-xia Yang and Shi-yong Yang

Additional information is available at the end of the chapter

http://dx.doi.org/10.5772/51182

## 1. Introduction

In advanced thin film transistor liquid crystal display devices (TFT-LCDs), alignment layers (ALs) are playing an ever-increasing important role for achieving a high-quality optoelectronic display [1]. The main function of AL materials is to align the rod-like liquid crystal (LC) molecules at a constant angle (so-called pretilt angle) to the local surface. Thus, when the electrical field is applied, the LC molecules can respond rapidly so as to result in a display effect. The characteristics of AL materials, including their abilities to achieve a proper pretilt angle for LC molecules, to achieve a high voltage holding ratio (VHR) and a low residual direct circuit voltage (RDC) value for the LCD devices, high thermal stability, high mechanical strength to resist rubbing process and their planarization ability are often taken into deliberate consideration in developing new generations of TFT-LCDs [2].

Currently, polyimides (PIs) are one of the most important AL materials for TFT-LCDs due to their intrinsic high thermal resistance, good mechanical properties and unique LC alignment ability [3]. However, conventional wholly aromatic PIs suffer from their poor solubility in common solvents. Thus, in practice, they can only be used in the form of soluble precursors, poly(amic acid)s (PAAs). For example, in conventional twisted nematic LCD (TN-LCD) and super-twisted nematic LCD (STN-LCD) fabrications, wholly aromatic PAA solution is first spin-coated onto an indium tin oxide (ITO) substrate, and then the solution is imidized at elevated temperatures up to 300 °C to form the imidized PI alignment layer. However, the

high curing temperature of PAAs often causes serious damage for the temperature-sensitive components in TFT-LCDs, such as the color filters which would be destroyed when the temperatures are higher than 230 °C [4]. Hence, PI alignment layers with low curing temperatures (<220 °C) have been developed in the past decades [5-7].

Besides the curing temperature consideration, the high VHR and low RDC values of the devices are also highly desired for advanced TFT-LCD fabrication in order to achieve a high-resolution display (high contrast, low image sticking, etc) [8]. VHR and RDC values of the TFT-LCD devices are influenced by many factors, including the characteristics of LC materials, the features of the PI alignment layers and the display modes of the devices. Among the factors, the effects of the chemical structures of the PI alignment layers are often critical. For instance, it has been well established that the highly conjugated molecular skeletons in wholly-aromatic PIs often lead to low VHR and high RDC values for the devices [9]. Thus, PI alignment layers with low conjugated structures have been paid increasing attentions.

Considering the above-mentioned structure-property relationship for PI alignment layers used for advanced TFT-LCDs, alicyclic or semi-alicyclic PIs have been confirmed to be the best candidates as AL materials up to now. Especially, semi-alicyclic PIs derived from alicyclic dianhydrides and aromatic diamines possess the best combined properties, including good thermal stability, good solubility in organic solvents, acceptable mechanical properties, good optical transparency, high VHR and low RDC values. Thus, semi-alicyclic PIs have been widely investigated as AL materials for advanced TFT-LCDs [10-12]. Figure 1 illustrates the developing trajectory of PI alignment layers with different kinds of display modes.

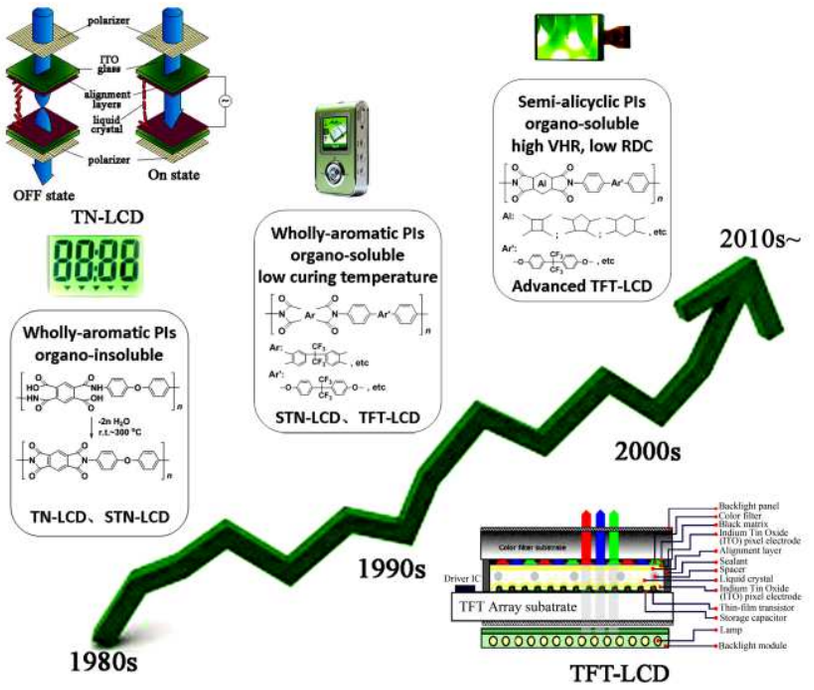


**Figure 1.** Developing trends of PI alignment layers for LCDs.

http://dx.doi.org/10.5772/51182

In this chapter, a series of novel semi-alicyclic PI alignment layers were designed and synthesized. The designed novel PI materials are expected to show good solubility in organic solvents (thus low curing temperatures) and exhibit high VHR and low RDC values for TFT-LCDs. For this purpose, a class of substituted-tetralin alicyclic dianhydrides was synthesized first via a low-cost route using maleic anhydride and substituted styrene compounds as the starting materials (Scheme 1). Then, a series of semi-alicyclic PIs were synthesized from the newly-developed dianhydrides and commercially available aromatic diamines. The effects of the structures of the semi-alicyclic PIs on their thermal stability and optical properties were investigated. At last, a series of test LCD cells with fringe field switching (FFS) mode were fabricated using the novel PIs as the alignment layers. The electrical characteristics (pretilt angle, VHR and RDC) of the cells were preliminarily studied.

## 2. Experiments

### 2.1. Materials

Styrene, *p*-methylstyrene, *p*-*tert*-butylstyrene and *p*-fluorostyrene were purchased from Tokyo Chemical Industry Co., Ltd., Japan (TCI) and used as received. It is unnecessary to remove the inhibitors in the chemicals. Maleic anhydride was obtained from Beijing Yili Fine Chemicals, China and used as received. 4,4'-Methylenedianiline (MDA, TCI, Japan) was recrystallized from ethanol and dried in vacuum at 80 °C overnight prior to use. 2,4-Diamino-(*n*-hexadecanoxy)benzene (16PDA) was synthesized in our laboratory and purified by continuous recrystallization from ethanol. Commercially available *N*-methyl-2-pyrrolidinone (NMP), *N*,*N*-dimethylacetamide (DMAc), cyclopentanone (CPA), γ-butyrolactone (GBL) and ethylene glycol monobutyl ether (butyl cellosolve, BC) were purified by distillation prior to use. The other commercially available reagents were used without further purification.

### 2.2. Measurements

Inherent viscosity was measured using an Ubbelohde viscometer with a 0.5 g/dL NMP solution at 25 °C. Absolute viscosity was measured using a Brookfield DV-II+ Pro viscometer at 25 °C. Fourier transform infrared (FT IR) spectra were obtained with a Tensor 27 Fourier transform spectrometer. Ultraviolet-visible (UV-vis) spectra were recorded on a Hitachi U-3210 spectrophotometer at room temperature. The cutoff wavelength was defined as the point where the transmittance drops below 1% in the spectrum. Prior to test, PI samples were dried at 100 °C for 1 h to remove the absorbed moisture. Yellow index (YI) and haze values of the PI films were measured using an X-rite color i7 spectrophotometer with PI film samples at a thickness of 30-40 μm in accordance with the procedure described in ASTM D1925 "Test method for yellowness index of plastics" and in ASTM D1003 "Standard test method for haze and luminous transmittance of transparent plastics", respectively. The color parameters were calculated according to a CIE Lab equation. $L^*$ is the lightness, where 100 means white and 0 implies black. A positive $a^*$ means a red color, and a negative one indicates a green color. A positive $b^*$ means a yellow color, and a negative one indicates a blue

color. Nuclear magnetic resonances ($^1$H NMR and $^{13}$C NMR) were performed on a AV 400 spectrometer operating at 400 MHz in DMSO-$d_6$ or $CDCl_3$. Differential scanning calorimetry (DSC) and thermogravimetric analysis (TGA) were recorded on a TA-Q series thermal analysis system at a heating rate of 10 °C/min and 20 °C/min in nitrogen or air, respectively. Gel permeation chromatography (GPC) measurements were performed using a Waters 1515 HPLC pump equipped with a Waters 2414 refractive index detector. Two Waters Styragel HR 4 columns kept at 35°C±0.1°C were used with HPLC grade NMP as the mobile phase at a flow rate of 1.0 mL/min. Number average weight ($M_n$), weight average molecular weight ($M_w$) and polydispersity ($M_w/M_n$) were then determined with polystyrene as a standard.

Solubility was determined as follows: 1.5 g of the PI resin was mixed with 8.5 g of the tested solvent at room temperature (15 wt% solid content), which was then mechanically stirred in nitrogen for 24 h. The solubility was determined visually as three grades: completely soluble (++), partially soluble (+), and insoluble (-). The complete solubility is defined as a homogenous and clean solution is obtained, in which no phase separation, precipitation or gel formation is detected.

The electrical characteristics, including VHR, RDC and pretilt angle values of the LC test cells were measured on a Toyo Model 6254 measurement system. VHR measurements were performed at LC test cells with a gap of 5-6 μm. The peak value of the square wave voltage and pulse duration was +5V and 60 μs, respectively. RDC measurements were performed using the "flick free" method. The test cells were first addressed with +5V direct circuit (DC) offset voltage for 3600 s. After the time, the +5V DC offset was switched off. The resulting flicker was monitored and the DC offset voltage was increased until the flickering was no longer visible. The compensating voltage was the residual DC voltage (RDC). Pretilt angles measurements were performed using the crystal rotation method with LC cells with a gap of 50 μm fabricated by anti-parallel rubbing process. The values of all measurements of VHR, RDC and pretilt angles are averages of at least 10 independent LC cells.

### 2.3. Monomer synthesis

*3,4-Dicarboxy-1,2,3,4-tetrahydro-6-methyl-1-naphthalene succinic dianhydride (MTDA).* Into a 500-mL three-necked flask equipped with a mechanical stirrer, a gas inlet and a condenser, 43.75 g (0.446 mol) of maleic anhydride, 80.60 g (0.682 mol) of *p*-methylstyrene, and 0.1138 g (0.5 mmol) of 2,5-di-*tert*-butyl hydroquinone were added. Nitrogen was introduced to remove the air in the system. Then, nitric oxide (NO) gas was introduced from a gas inlet placing under the surface of the reaction solution. The reaction mixture were heated to 120°C and maintained for 5 h under an atmosphere of nitric oxide. The produced red-brown nitrogen oxide gas was trapped by passing through an aqueous solution of 20 wt% sodium hydroxide. An orange precipitate formed during the reaction. After the reaction, the mixture was cooled to room temperature and 60 ml of acetonitrile was then added. The reaction mixture was heated to reflux for another 0.5 h. Then, 60 ml of toluene was added and the reaction mixture was cooled to temperature. The produced white needle crystals were collected by filtration and the solid was washed with toluene and petroleum ether in succession. After

being dried in vacuum at 80 °C for 24h, the pure MTDA was obtained as white crystals. Yield: 51.44 g (73.4%).

Melting point: 229 °C (DSC peak temperature). FT IR (KBr, $cm^{-1}$): 2941, 1855, 1778, 1506, 1412, 1223, 1076, and 916. $^1$H NMR (DMSO-$d_6$, ppm): 7.35 (*s*, 1H), 7.15-7.13 (*m*, 1H), 7.10-7.09 (*m*, 1H), 4.56-4.54 (*d*, 1H), 4.12-4.10 (*m*, 1H), 3.83-3.81 (*m*, 1H), 3.18-3.13 (*m*, 1H), 3.09 (*m*, 1H), 2.82-2.78 (*m*, 1H), 2.32 (*s*, 3H), 1.97-1.95 (*m*, 1H), and 1.86-1.85 (*m*, 1H). $^{13}$C NMR (DMSO-$d_6$, ppm): 175.8, 175.3, 173.8, 172.4, 138.1, 135.0, 131.8, 130.5, 129.9, 127.7, 45.1, 44.2, 36.4, 32.3, 26.4, and 22.0. MS (EI, m/e, percentage of relative intensity): 142 ($M^+$-172, 100). Elemental analysis: calculated for $C_{17}H_{14}O_6$: C, 64.97%, H, 4.49%; Found: C, 64.32%, H, 4.44%.

*3,4-Dicarboxy-1,2,3,4-tetrahydro-1-naphthalene succinic dianhydride (TDA).* The dianhydride was synthesized from styrene and maleic anhydride through a similar route to MTDA. The product was obtained as white crystals. Yield: 50.35 g (75.2%).

Melting point: 199 °C (DSC peak temperature). FT IR (KBr, $cm^{-1}$): 2966, 1861, 1780, 1493, 1405, 1229, 1058, and 928. $^1$H NMR (DMSO-$d_6$, ppm): 7.69-7.67 (*d*, 1H), 7.38-7.27 (*m*, 2H), 7.20-7.19 (*d*, 1H), 4.67-4.64 (*d*, 1H), 3.73-3.58 (*m*, 2H), 3.40-3.33 (*m*, 1H), 2.85-2.80 (*m*, 2H), and 2.12-2.07 (*m*, 2H). $^{13}$C NMR (DMSO-$d_6$, ppm): 173.8, 173.5, 172.1, 170.8, 136.4, 129.5, 128.4, 128.1, 127.5, 127.4, 42.8, 42.1, 37.3, 36.7, 32.8, and 26.2. MS (EI): 128 ($M^+$-172, 100). Elemental analysis: calculated for $C_{16}H_{12}O_6$: C, 64.00%, H, 4.03%; Found: C, 64.10%, H, 4.03%.

*3,4-Dicarboxy-1,2,3,4-tetrahydro-6-tert-butyl-1-naphthalene succinic dianhydride (TTDA).* The dianhydride was synthesized from *p-tert*-butylstyrene and maleic anhydride through a similar route to MTDA. The product was obtained as white crystals. Yield: 58.49 g (73.6%).

Melting point: 218 °C (DSC peak temperature). FT IR (KBr, $cm^{-1}$): 2962, 1859, 1789, 1504, 1410, 1222, 1055, and 925. $^1$H NMR (DMSO-$d_6$, ppm): 7.70 (*s*, 1H), 7.34-7.32 (*d*, 2H), 7.13-7.11 (*d*, 1H), 4.65-4.62 (*d*, 1H), 3.74-3.67 (*m*, 1H), 3.62-3.58 (*m*, 1H), 3.31-3.30 (*m*, 1H), 2.93-2.76(*m*, 2H), 2.44-2.39(*m*, 1H), 2.13-2.07 (*m*, 1H) and 1.29(*s*, 9H). $^{13}$C NMR (DMSO-$d_6$, ppm): 174.4, 174.0, 172.7, 171.3, 150.2, 134.0, 128.4, 128.1, 126.6, 125.0, 43.3, 42.8, 38.0, 36.8, 34.7, 33.3, 31.5, and 26.8. MS (EI): 239 ($M^+$-118, 100). Elemental analysis: calculated for $C_{20}H_{20}O_6$: C, 67.41%, H, 5.66%; Found: C, 67.23%, H, 5.70%.

*3,4-Dicarboxy-1,2,3,4-tetrahydro-6-fluoro-1-naphthalene succinic dianhydride (FTDA).* The dianhydride was synthesized from *p*-fluorostyrene and maleic anhydride through a similar route to MTDA. The product was obtained as white crystals. Yield: 55.60 g (77.3%).

Melting point: 201 °C (DSC peak temperature). FT IR (KBr, $cm^{-1}$): 2912, 1864, 1782, 1664, 1441, 1376, 1304, 1262, 1211, 1151, 1080, 1027, 967, 914, 870, 819, 754, 633, 594, 558 and 498. $^1$H NMR (DMSO-*d6*, ppm): 7.51-7.49 (*d*, 1H), 7.29-7.27 (*m*, 2H), 7.17-7.14 (*m*, 1H), 4.69-4.68 (*d*, 1H), 3.75-3.71 (*m*, 1H), 3.60-3.57(*m*, 1H), 3.44-3.43(*m*, 1H), 2.85-2.83 (*m*, 2H), 2.57-2.53(*m*, 1H) and 2.10-2.06 (*m*, 1H). $^{13}$C NMR (DMSO-$d_6$, ppm): 173.9, 172.3, 171.2, 162.3, 160.7, 133.1, 131.3, 130.6, 116.2, 114.9, 43.3, 42.4, 37.3, 36.7, 33.2 and 26.5. MS (EI): 146 ($M^+$-172, 100). Elemental analysis: calculated for $C_{16}H_{11}FO_6$: C, 60.38%, H, 3.48%; Found: C, 59.90%, H, 3.53%.

### 2.4. Polyimide synthesis

The general procedure for the synthesis of PIs can be illustrated by the preparation of PI-8 (Table 1). Into a 250 mL three-necked, round-bottomed flask equipped with a mechanical stirrer, a Dean-Stark trap and a nitrogen inlet, MDA (17.8434 g, 0.09 mol) and 16PDA (3.457 g, 0.01 mol) was dissolved in *m*-cresol (100 g) to give a clear diamine solution. Then, FTDA (31.825 g, 0.1 mol) was added in one batch and an additional volume of *m*-cresol (112 g) was added to wash the residual dianhydride, and at the same time to adjust the solid content of the reaction system to be 20 wt%. After stirring in nitrogen for 1 h, a mixture of toluene (230 ml) and isoquinoline (catalytic amount) was then added. The reaction mixture was heated to 180 °C and maintained for 6 h. During the reaction, the toluene-water azeotrope was distilled out of the system and collected in the Dean-Stark trap. After cooling to room temperature, the viscous solution was slowly poured into an excess of ethanol to yield a silky resin. The resin was collected and dried at 80 °C in vacuo for 24 h. Yield: 47.54 g (96%).

PI-8 resin (15 g) was dissolved in NMP (85 g) at room temperature to afford a 15 wt% solution. The solution was filtered through a 0.45 μm Teflon syringe filter to remove any undissolved impurities. Then, the solution was spin-coated on a clean silicon wafer or quartz substrate. The thickness of the PI film was controlled by regulating the spinning rate. PI-8 films with thicknesses ranged from 10~100 μm were obtained by thermally baking the solution in a flowing nitrogen according to the following heating procedure: 80 °C/2 h, 150 °C/1 h, 200 °C/1 h, and 220 °C/1 h. The other PI resin and films were prepared according to a similar procedure as mentioned above.

## 3. Results and discussion

### 3.1. Monomer synthesis

Scheme 1 illustrates the synthetic procedure for the substituted-tetralin alicyclic dianhydrides. Four dianhydrides, including TDA (*R*=-H), MTDA (*R*=-$CH_3$), TTDA (*R*=-$C(CH_3)_3$) and FTDA (*R*=-F) were synthesized by the Diels-Alder reactions of *R*-substituted-styrene compounds and maleic anhydride followed by the rearrangement reactions of the intermediates. The yields are all higher than 70%. The styrene compounds were used as both of the reactant and the solvent. In the literature, TDA has been synthesized from styrene and maleic anhydride with a molar ratio of 2.1:1 [13]. Toluene and a flowing air (15 liters per hour) were used as the solvent and catalyst, respectively. The obtained TDA dianhydride needed to be purified by recrystallization from a toluene/acetone mixture to remove the oxidized by-products. In our experiments, the reductive nitric oxide (NO) gas was used instead of the oxidative air. The obtained dianhydrides have good purity and can be used directly for polymerization. Also, they can be further purified by dissolution in a good solvent of acetonitrile and then precipitated slowly by adding a poor solvent of toluene although the yields might be slightly sacrificed. Due to the low cost of the starting materials and the high synthesizing yields for the new dianhydrides, this route is a promising procedure reducing the high cost of the present alicyclic PI alignment layers (usually hundreds of dollars per li-

http://dx.doi.org/10.5772/51182

ter). In addition, this reaction is easily to expand to a large scale. A scale of kilograms per batch has been successfully achieved in our lab.

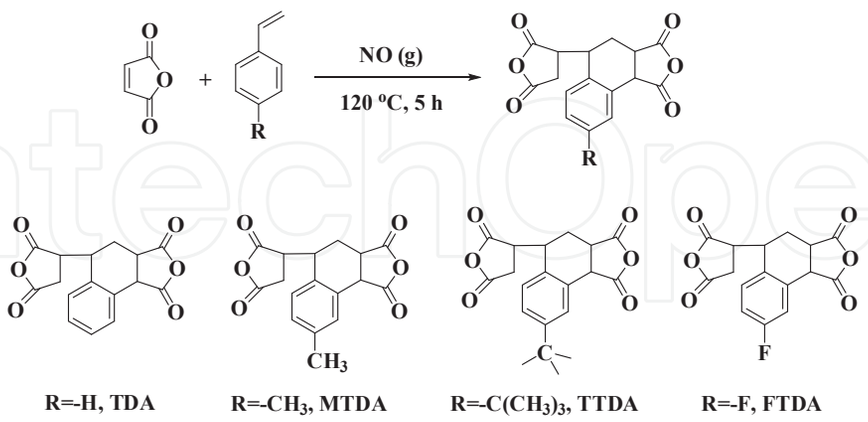


**Scheme 1** Synthesis of new alicyclic dianhydrides via a low-cost route

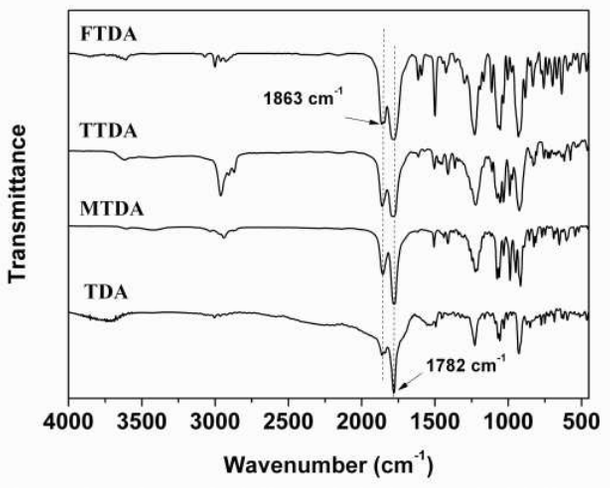


**Figure 2.** FT IR spectra of tetralin dianhydrides

Figure 2 shows the FT IR spectra of the dianhydrides, in which the characteristic bands of carbonyl groups in the anhydride moiety were clearly observed at around 1863 and 1782 $cm^{-1}$ for all of the compounds. In addition, the characteristic absorption of methyl group appeared at 2941 $cm^{-1}$ for MTDA and TTDA. The $^{13}C$ NMR and the two-dimensional $^{1}H$-$^{13}C$ heteronuclear single-quantum coherence (HSQC) spectra of TTDA and FTDA are illustrated in Figure 3, together with the assignments of the observed resonances. As depicted in Figure 3, 18 carbon signals are clearly revealed for TTDA and 15 signals for FTDA. The absorptions of the protons cohered well with those of the corresponding carbon signals. This result is consistent with their proposed structures. Interestingly, the two pairs of protons in methylene groups ($H_{3,3'}$ and $H_{6,6'}$) for both of the dianhydrides exhibited individual absorptions in

their $^{1}H$ NMR spectra due to the slightly different chemical environments of the protons in the dianhydrides. The protons in the aromatic ring ($H_{13}$, $H_{14}$, and $H_{16}$) appeared at the lowest field in the spectra. In addition, elemental analysis results also revealed the successful preparation of the target dianhydrides.

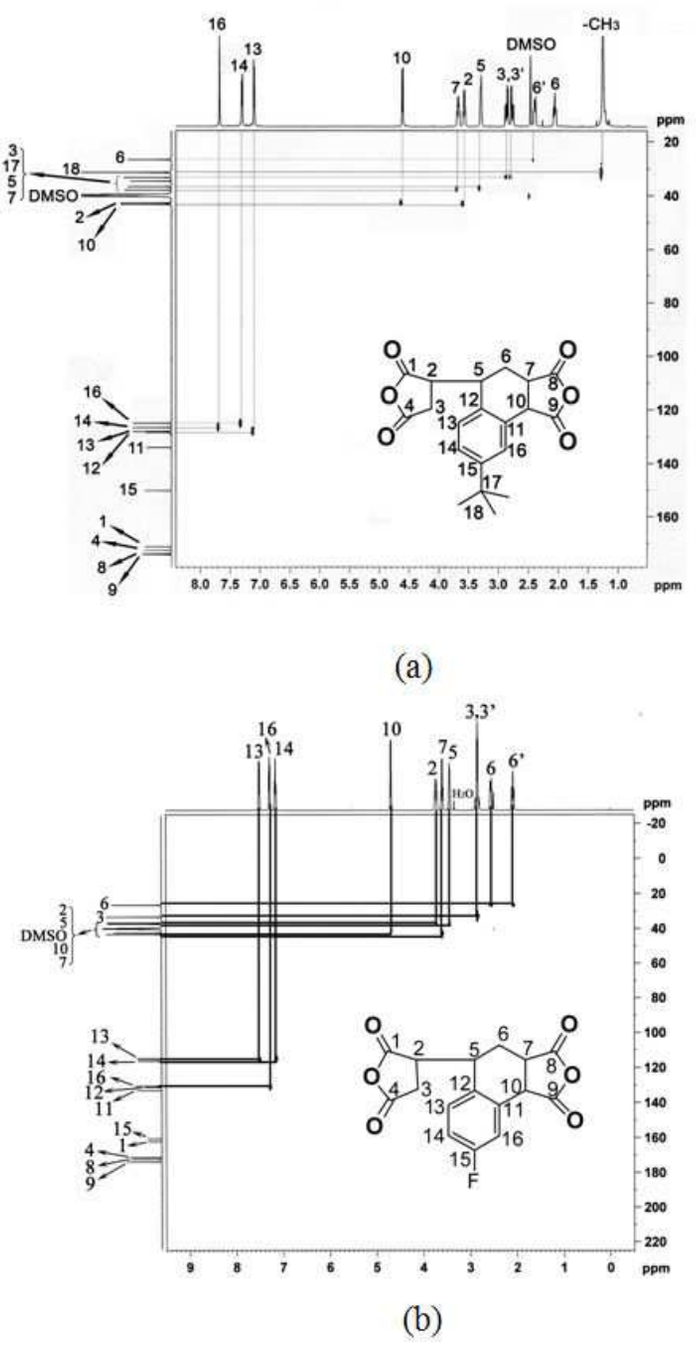


**Figure 3.** $^{1}H$-$^{13}C$ HSQC spectra of dianhydrides (a) TTDA; (b) FTDA.

http://dx.doi.org/10.5772/51182

### 3.2. Polyimide synthesis

As shown in Scheme 2, three series, totally 9 species of PIs were designed and synthesized from TDA (PI-1~PI-3), MTDA (PI-4~PI-6), FTDA (PI-7~PI-9) and aromatic diamines (MDA and 16PDA) by a one-step, high temperature polycondensation procedure in *m*-cresol solution at a temperature of 180 °C. Introduction of $C_{16}$ long alkyl chain in the PI systems is mainly to induce the alignment of LC molecules [14-16]. The reaction proceeded smoothly during the polymerization, indicating good solubility of the reactants and the yielded PIs in the solvents.

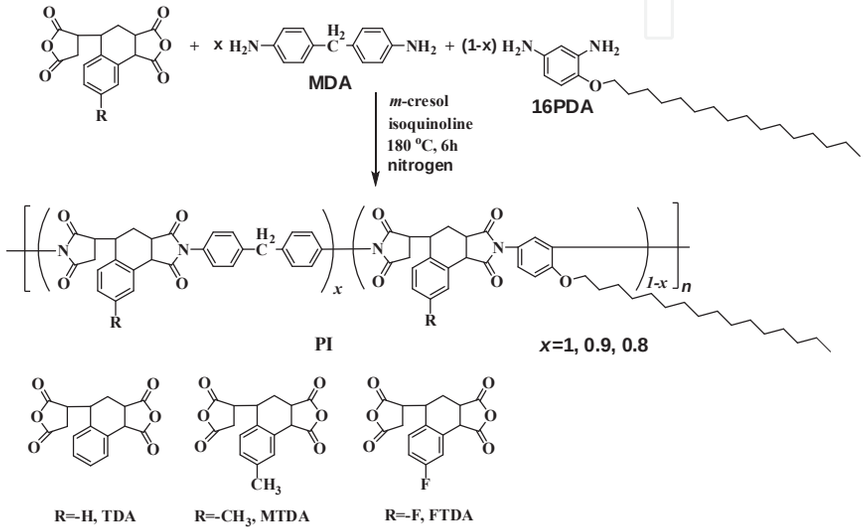


**Scheme 2.** Synthesis of semi-alicyclic PIs

Table 1 presents the chemical formulations, inherent viscosities and molecular weights of the obtained PIs. The utilization of high temperature polycondensation procedure in the present work is mainly based on the fact that the two anhydride moiety in the substituted-tetralin dianhydrides might exhibit different reactivities due to the asymmetrical molecular structures of the monomers. High polymerization temperatures might eliminate the reactivity differentia of the anhydride units so as to obtain the PI resins with higher molecular weights. White or pale-yellow fibrous PI resins were obtained quantitatively, which had inherent viscosities of 0.81~1.03 dL/g for TDA-PIs (PI-1~3), 0.76~1.04 dL/g for MTDA-PIs (PI-4~6) and 0.69~0.97 dL/g for FTDA-PIs (PI-7~9), respectively (Table 1). These values indicate that the current PIs possess moderate to high molecular weights, which can be further confirmed by the GPC measurements. As tabulated in Table 1, the average numerical ($M_n$) and weight ($M_w$) molecular weights of the PI resins were higher than 17762 g/mol and 35356 g/mol, respectively. In addition, the PI resins exhibited a polydispersity index ($M_w/M_n$) lower than 2.43. This indicates that the substituted-tetralin alicyclic dianhydrides exhibited good reactivity in polymerization with aromatic diamines. Flexible and tough PI films were obtained by casting their solutions in NMP followed by baking at elevated temperatures from 80-220°C. All the films exhibited creasable nature and good tensile properties. For instance, PI-8 showed a tensile strength of 76 MPa, an elongation at break of 6.2%, and a ten-

sile modulus of 2.2 GPa. Figure 4 presents the free-standing (left) and creased appearance of PI-8 film at a thickness of 25 μm.

| PI | Dianhydride | Diamine (mol %) | | $[\eta]_{inh}$* (dL/g) | Molecular weight (g/mol) | | |
|---|---|---|---|---|---|---|---|
| | | MDA | 16PDA | | $M_n$ | $M_w$ | $M_w/M_n$ |
| PI-1 | TDA | 100 | 0 | 1.03 | 31,326 | 73,798 | 2.36 |
| PI-2 | | 90 | 10 | 0.90 | 22,319 | 53,387 | 2.39 |
| PI-3 | | 80 | 20 | 0.81 | 17,762 | 36,715 | 2.07 |
| PI-4 | MTDA | 100 | 0 | 1.04 | 30,321 | 68,823 | 2.27 |
| PI-5 | | 90 | 10 | 0.94 | 25,319 | 61,528 | 2.43 |
| PI-6 | | 80 | 20 | 0.76 | 18,463 | 35,729 | 1.94 |
| PI-7 | FTDA | 100 | 0 | 0.97 | 33,192 | 80,281 | 2.42 |
| PI-8 | | 90 | 10 | 0.88 | 27,834 | 57,339 | 2.06 |
| PI-9 | | 80 | 20 | 0.69 | 20,121 | 35,356 | 1.76 |

* $[\eta]_{inh}$: inherent viscosity measured with a PI resin at a concentration of 0.5 g/dL in NMP at 25 °C.

**Table 1.** Inherent viscosities and molecular weights of the PIs

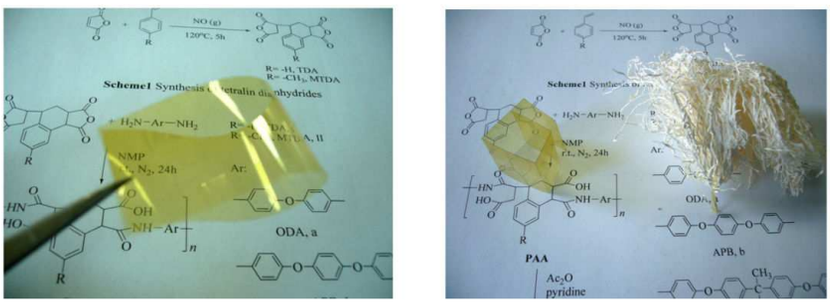


**Figure 4.** Appearance of PI-8 film (left) and resin (right)

Figure 5 illustrates the typical FT IR spectra of the PIs. It can be obviously observed that the characteristic absorptions of imide moiety at 1778 and 1711 $cm^{-1}$, due to the asymmetric and symmetric carbonyl stretching vibrations of the imide groups, and the absorptions at 1383 $cm^{-1}$ assigned to the C-N stretching vibration of the imide structure are observed in all of the PIs. Typical $^1H$ NMR spectra of PI-7 and PI-8 are shown in Figure 6. For both of the PIs, the spectra are clearly divided into two parts. One part is the aliphatic, alicyclic and methylene protons in the upfield region; the other part is the aromatic protons in dianhydride moiety ($H_9$, $H_{10}$ and $H_{11}$) and diamine moiety ($H_{12}$ and $H_{13}$) in the lowfield region. Similarly, the two pairs of protons in methylene groups ($H_{2,3}$ and $H_{5,6}$) exhibited individual absorptions in the spectra due to the different chemical environments of the protons in the polymers. For PI-8,

the absorptions of $C_{16}$ long alkyl chain protons are obviously observed at 0.83 ppm, 1.21 ppm, 1.89 ppm and 3.42 ppm, respectively, although some of the absorptions are overlapped by the absorptions of tetralin protons. In addition, the resonances observed at around 6.80 ppm ($H_{15}$, $H_{16}$ and $H_{17}$) assigned to the absorptions of aromatic ring protons in 16PDA moiety proved the successful preparation of the target polymer.

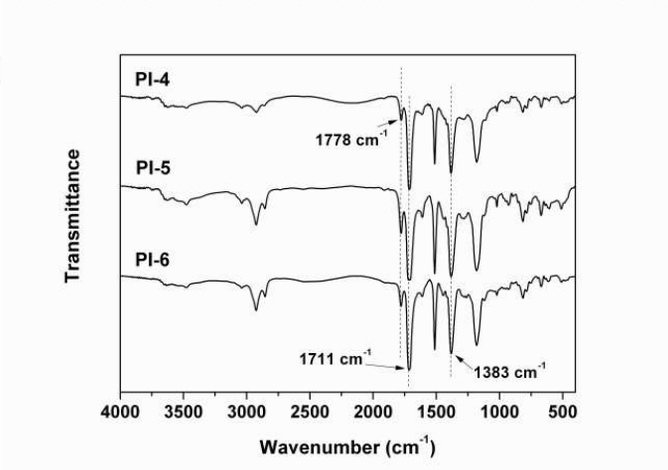


**Figure 5.** FT IR spectra of MTDA-PIs (PI-4~PI-6)

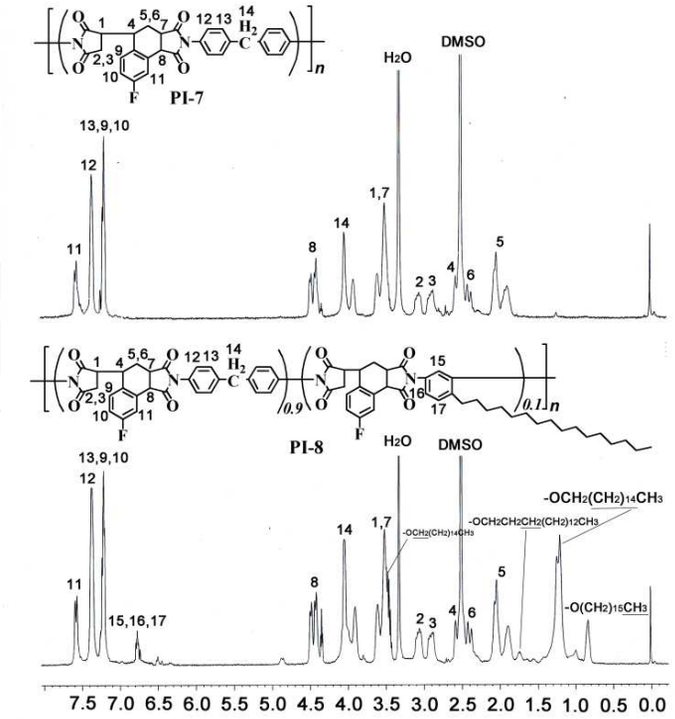


**Figure 6.** NMR spectra of PI-7 and PI-8

### 3.3. Solubility

The solubility of PIs is summarized in Table 2. All the PIs were easily soluble in polar aprotic solvents (NMP and DMAc), *m*-cresol, and γ-butyrolactone (GBL) at a concentration of 15 wt%. Among the PIs, those derived from MTDA (PI-4~PI-6) showed the best solubility due to the synergic effects of bulky tetralin moiety and pendant methyl substituent in the dianhydride unit, and flexible alkyl side chains in the diamine unit. PI-5 and PI-6 were even wholly soluble in dichloromethane at room temperature. In the same condition, the PIs derived from TDA or FTDA were only partially or not soluble in dichloromethane. The enhancement of the solubility of MTDA-PIs can be attributed to the more loose packing of the molecular chains induced by the substituents mentioned above.

| PI | Solvent | | | | | | |
|---|---|---|---|---|---|---|---|
| | NMP | DMAc | γ-BL | BC | *m*-cresol | THF | $CH_2Cl_2$ |
| PI-1 | ++ | ++ | ++ | — | ++ | — | — |
| PI-2 | ++ | ++ | ++ | — | ++ | — | + |
| PI-3 | ++ | ++ | ++ | — | ++ | — | + |
| PI-4 | ++ | ++ | ++ | — | ++ | — | + |
| PI-5 | ++ | ++ | ++ | — | ++ | — | ++ |
| PI-6 | ++ | ++ | ++ | — | ++ | — | ++ |
| PI-7 | ++ | ++ | ++ | — | ++ | — | — |
| PI-8 | ++ | ++ | ++ | — | ++ | — | + |
| PI-9 | ++ | ++ | ++ | — | ++ | + | + |

* ++: Wholly soluble at room temperature; +: Partially soluble; —: Insoluble; NMP: *N*-methyl-2-pyrrolidinone; DMAc: *N,N*-dimethylacetamide; GBL: γ-butyrolactone; BC: ethylene glycol monobutyl ether.

**Table 2.** Solubility of the PIs*

The effects of solid contents ($S_c$) on the viscosities ($\eta$) of the PIs were further investigated. This investigation is very important for applications of the PIs as alignment layers for TFT-LCDs because a proper $S_c$-$\eta$ relationship for PI would be beneficial for its orientation to LC molecules. Figure 7 illustrates the correlations between the absolute viscosities and solid contents of PI-2, PI-5 and PI-8 solution in NMP. Although these three PIs were all soluble in NMP, the $\eta$ values of the solutions were quite different. For instance, at the same solid content of 35 wt%, PI-2 had a $\eta$ value of 26750 mPa.s, which was much lower than those of PI-5 (64440 mPa.s) and PI-8 (116000 mPa.s). Thus, in practical application, PI-2 is more suitable to be utilized to develop a soluble PI solution with a high solid content and at the same time a relatively low viscosity. However, for the applications as alignment layers for TFT-LCDs, in which the solid content of the PIs are usually lower than 15 wt%, all of the PIs developed in

this work might be suitable because they all exhibit a relatively low absolute viscosities at a solid content of 15 wt% (PI-2: 150 mPa.s; PI-5: 200 mPa.s; PI-8: 160 mPa.s).

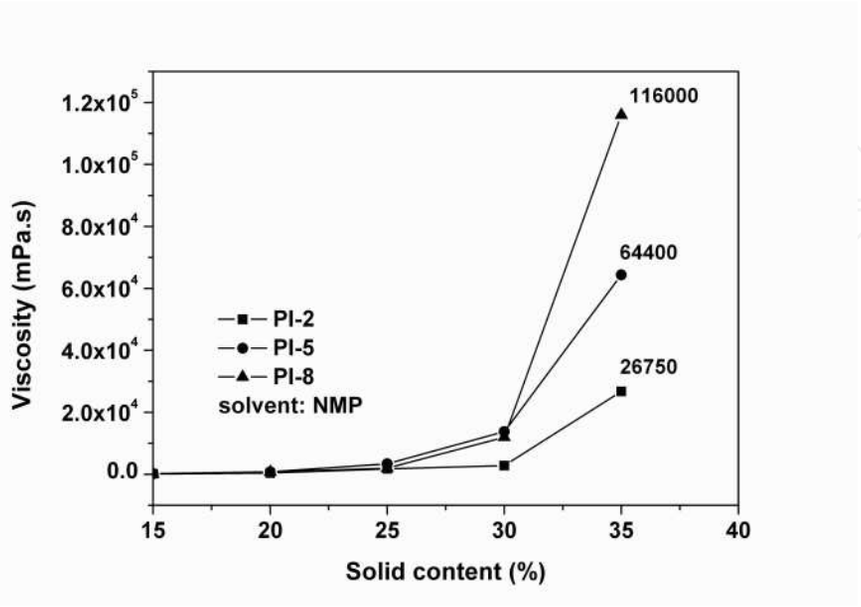


**Figure 7.** Viscosities as a function of solid contents for PI-2, PI-5 and PI-8 in NMP.

### 3.4. Thermal properties

The effects of asymmetrical *R*-substituted tetralin structure in the dianhydride units and the $C_{16}$ long alkyl side chains in the diamine moieties on the thermal stabilities of the PIs were investigated by TGA and DSC measurements. Table 3 summarizes the thermal characterization of the polymers. Figure 8 depicts the thermogravimetry plots of PI films over a temperature range of 50 to 750 °C in nitrogen and PI-2 in nitrogen and in air. It can be seen from Figure 8a that the current PIs possess good thermal stability with no significant weight loss up to approximately 400 °C. After 400 °C, the PIs lose their original weight rapidly, leaving a residual weight ratio in the range 1.8-32.7% at 600 °C. The 10% weight loss temperatures ($T_{10\%}$) of the PIs are all higher than 410 °C in nitrogen. This implies that the incorporation of aliphatic or alicyclic moiety in the PIs did not apparently sacrifice their thermal stability. Among the series, FTDA-PIs (PI-7~PI-9) exhibited the best thermal stability, which might be due to the higher bond energy of C-F compared to those of C-H (TDA) and C-C (MTDA). As can be seen form Figure 8a that the PIs exhibited single-stage thermal decomposition behaviors in nitrogen. However, they showed a two-stage thermal decomposition in air, as can be depicted in Figure 8b. For example, PI-2 showed a first thermal decomposition at about 400 °C in air. When the temperature increased, a second thermal decomposition occurred at 580 °C. The first thermal decomposition might be due to the oxidative cleavage of the $C_{16}$ long alkyl side chains at elevated temperature and the second one was attributed to the decomposition of the residual molecular skeleton of PI-2. Although the thermal stability of the cur-

rent PIs is lower than that of common aromatic PIs (usually with a $T_{10\%}$ values >500 °C), it is high enough for their applications in TFT-LCD fabrications.

| PI | $T_g$ (°C) | $T_{5\%}$(°C) | $T_{10\%}$ (°C) | $R_{w600}$ (%) |
|---|---|---|---|---|
| PI-1 | 235 | 399 | 422 | 5.3 |
| PI-2 | 257 | 420 | 436 | 1.8 |
| PI-3 | 233 | 407 | 425 | 6.7 |
| PI-4 | 244 | 412 | 434 | 13.3 |
| PI-5 | 261 | 428 | 447 | 8.5 |
| PI-6 | 252 | 396 | 414 | 16.0 |
| PI-7 | 248 | 408 | 427 | 22.6 |
| PI-8 | 270 | 428 | 441 | 24.2 |
| PI-9 | 225 | 390 | 411 | 32.7 |

* $T_g$: glass transition temperature; $T_{5\%}$, $T_{10\%}$: temperatures at 5% and 10% weight loss, respectively; $R_{w600}$: residual weight ratio at 600 °C in nitrogen.

**Table 3.** Thermal properties of PI films

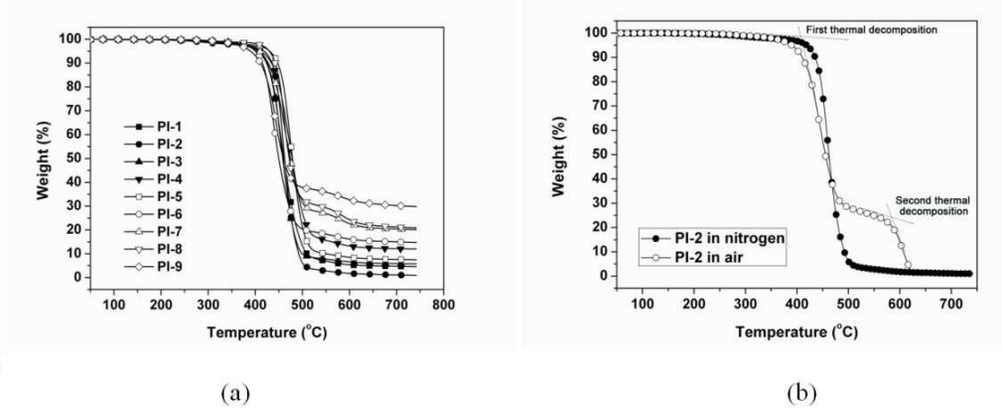


**Figure 8.** TGA curves of PI films. (a) PI films in nitrogen; (b) PI-2 in nitrogen and in air

Glass transition temperatures ($T_g$) values were obtained from the second heating scans of PI samples at a heating rate of 10 °C /min in nitrogen. The data were summarized in Table 3 and the typical DSC curves of FTDA-PIs are shown in Figure 9. All the PIs exhibit good thermal stabilities with the $T_g$ values in the range of 233~270℃, depending on the rigidity of the polymers. It is observed that for the same dianhydride, PI containing 10% molar ratio of 16PDA exhibited the highest $T_g$ values. For example, PI-2, PI-5 and PI-8 showed $T_g$ values of 257 °C, 261 °C and 270 °C, respectively, which were all the highest one among their series. This indicates that introduction of 16PDA at a low proportion, such as 10%, can increase the

$T_g$s of the PIs due to the rigid nature of *meta*-phenylenediamine skeleton in the diamine; however, overloading of the diamine would conversely decrease the $T_g$s of the PIs due to the flexible long alkyl chains and ether linkage in the diamine.

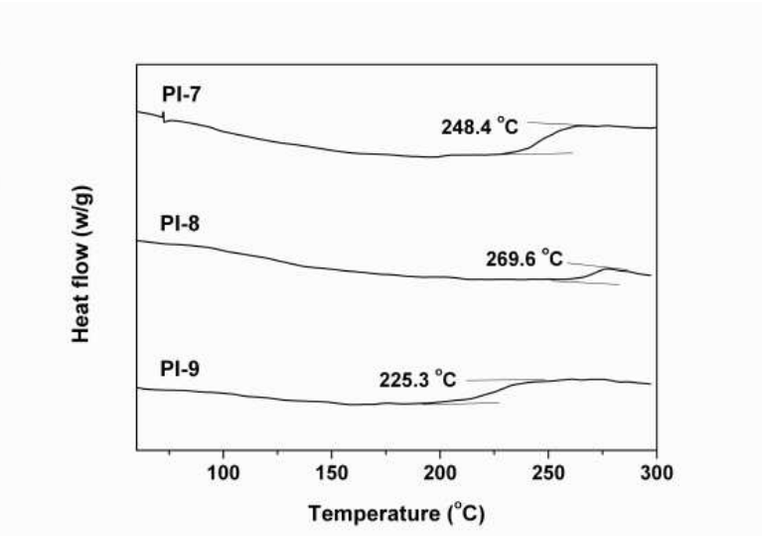


**Figure 9.** DSC curves of the FTDA-PI films (10 °C/min, in nitrogen)

| PI | λ (nm) | $T_{450}$ (%) | $a^*$ | $b^*$ | $L^*$ | Haze | YI |
|---|---|---|---|---|---|---|---|
| PI-1 | 319 | 66.7 | -2.80 | 17.46 | 92.06 | 2.50 | 29.32 |
| PI-2 | 302 | 82.7 | -1.74 | 7.84 | 94.31 | 5.85 | 13.39 |
| PI-3 | 331 | 52.3 | —** | — | — | — | — |
| PI-4 | 304 | 79.4 | -2.76 | 12.02 | 93.76 | 1.86 | 19.90 |
| PI-5 | 298 | 82.0 | -2.05 | 10.10 | 94.11 | 2.03 | 17.07 |
| PI-6 | 306 | 78.5 | -3.63 | 21.98 | 92.42 | 1.69 | 35.76 |
| PI-7 | 299 | 82.2 | — | — | — | — | — |
| PI-8 | 297 | 84.3 | -1.30 | 7.71 | 94.56 | 0.78 | 13.26 |
| PI-9 | 303 | 81.4 | — | — | — | — | — |

* λ: cutoff wavelength; $T_{450}$: transmittance at 450 nm; $a^*$, $b^*$, $L^*$: see 2.2 measurement; ** ND: not detected.

**Table 4.** Optical transparency and yellow indices of PI films*

### 3.5. Optical properties

It has been well established in the literature that the optical transparency of aromatic PI films can be efficiently improved by decreasing the formation of intra- and intermolecular charge transfer complexes (CTC) in the PI chains [17, 18]. When elaborately designed, color-

less PI films can even be obtained [19-21]. Among various methodologies decreasing the CTC formations, introduction of alicyclic moiety either in the dianhydride or in the diamine moiety has been proven to be one of the most effective procedures.

In the present work, the tetralin-containing PI films were obtained as pale-yellow free-standing films. The optical properties of the films are summarized in Table 4 and the UV-Vis spectra of the MTDA-PI films are illustrated in Figure 10. The PI films showed good optical transparency in the ultraviolet-visible light region with cutoff wavelengths lower than 300 nm. Some of the PI films, such as those derived from FTDA showed transmittances around 80% at 450 nm wavelength at a thickness of 10 μm. The good optical transparency of the PI films, on one hand, is attributed to the asymmetrical and bulky alicyclic tetralin structure in the dianhydride unit through steric hindrance. On the other hand, the high electronegativity of fluoro substituents in the dianhydride moiety is also beneficial for improving the optical transparency of the PI films by reducing the CTC formation.

The yellow index (YI) measurement results are shown in Table 4 and Figure 11. YI is usually adopted as a criterion evaluating the color of a polymer film. This value describes the color change of a film sample form clear or white toward yellow. Lower YI value usually indicates a weak coloration for a polymer film [22]. As shown in Table 5, PI-8 exhibited the lowest YI and Haze values compared with its analogs. This result correlated well with the results measured by UV-Vis measurements.

In summary, this low-color feature for the current PI films is desirable for their application as alignment layers for TFT-LCDs.

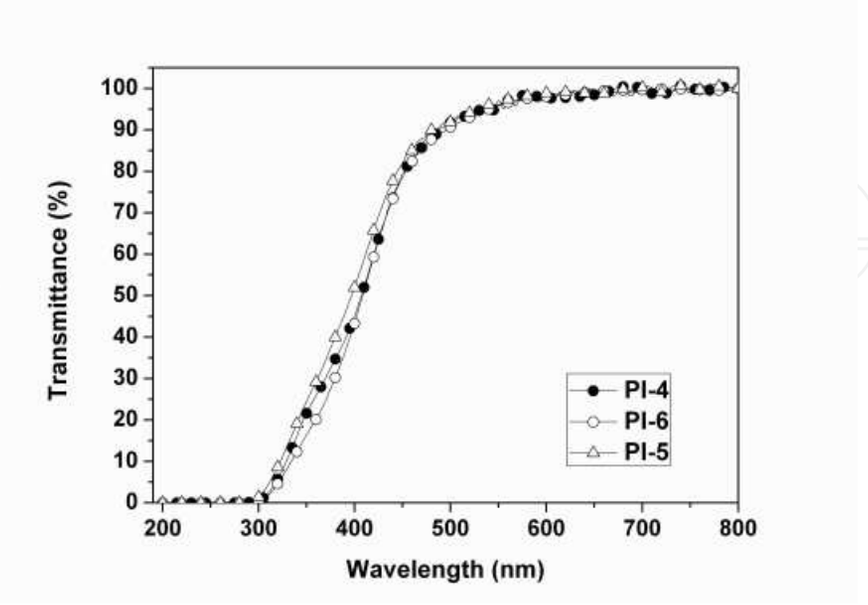


**Figure 10.** UV-Vis spectra of PI films derived from MTDA (PI-4~PI-6)

http://dx.doi.org/10.5772/51182

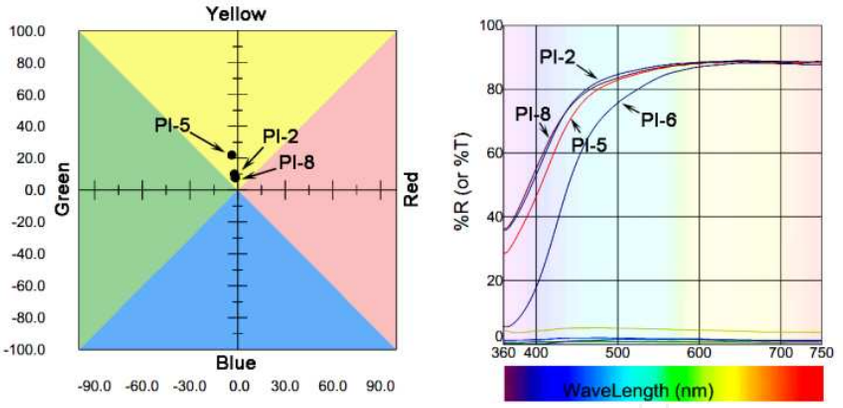


**Figure 11.** Yellow indices of PI films

### 3.6. Application in TFT-LCD fabrication

In order to investigate the practical application of the newly-developed alicyclic PIs as alignment layers for TFT-LCDs, a series of fringe field switching (FFS) mode [23, 24] liquid crystal cells (FFS-LCDs) were fabricated. PI-8 was chosen as the alignment layer due to its good combined properties. Figure 12 illustrates the LC cells fabrication procedure form monomer synthesis to devices.

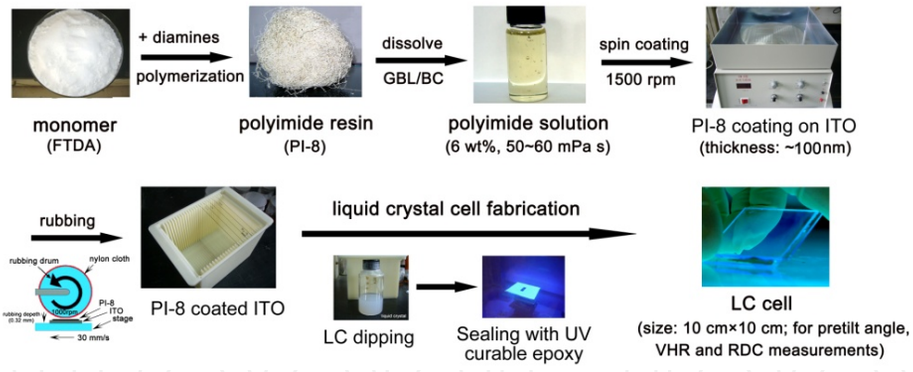


**Figure 12.** LC cells fabrication procedure from monomer synthesis to devices

First, PI-8 resin was dissolved in a mixture solvent of NMP/GBL/BC (55/30/15, volume ratio) at a solid content of 6.0 wt%. BC (butyl cellosolve) was used in the mixed solvents as a planarization agent so as to obtain a uniform PI coating. The obtained PI-8 solution was purified by filtering through a 0.25 μm Teflon filter and had a viscosity of 55 mPa·s. The purified PI-8 solution was spin-coated on an ITO glass substrate (10 cm×10 cm) at a rotating speed of 3000 rpm. Then the ITO glasses with PI-8 coating were placed on a hot plate at 80 °C for 30 min, followed by curing in a nitrogen oven at 230 °C for 1h. The thicknesses of PI-8 film was measured with a profilometer (Dektak XT, Bruker) and found to be 553.7 Å, as shown in Figure 13.

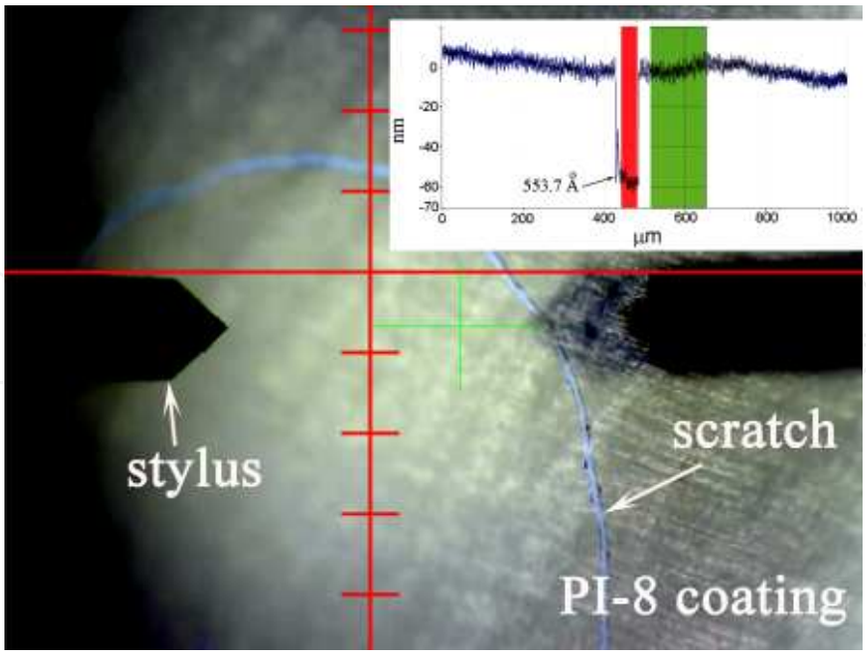


**Figure 13.** Thickness of PI-8 alignment layer

The cured PI-8 film was then rubbed with a nylon cloth-packed rubbing roller using the following parameters: radius of rubbing roller: 50 mm; rotation speed: 1000 rpm; pile impression: 0.32 mm and stage speed: 30 mm/s. Then, the FFS-LCD cells were assembled by two individual rubbed ITO glasses and the rubbing direction of the two glasses was anti-parallel to each other. For the pretilt angle measurements, the cell thickness was controlled to be about 50 μm by spraying spacers or glass fibers (50 μm) on PI-8 film surface; whereas for VHR and RDC measurements, the thickness was about 6 μm. The fabricated LC cells were sealed with a UV-curable epoxy sealant with two small filling holes left. LC molecules were then filled into the filling holes between the ITO plates via capillary action. The rod like LC molecules are thought to be oriented along the long alkyl chains pre-aligned by the rubbing treatments [25], as illustrated in Figure 14.

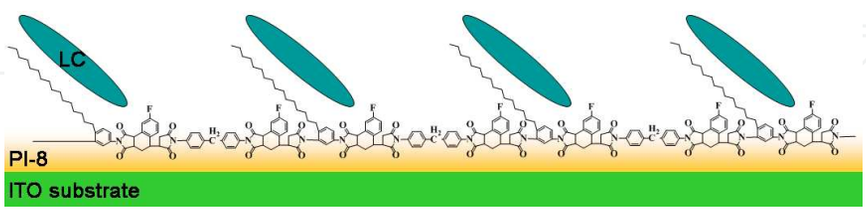


**Figure 14.** Schematic diagram of LC alignment on PI surfaces

Table 5 tabulates the electrical properties of the fabricated LC cells. The LC cells exhibited an average pretilt angle of 2.7°, which could meet the demands of the FFS-LCD applications. Meanwhile, a VHR of 98.2% and a RDC of 230 mV were also obtained. This result indicated that PI-8 alignment layer could endow the LC cells with a high VHR level; however, a few

charge accumulations occurred in the LC cells. The RDC value of 230 mV is a bit higher than the desired value (<100 mV) for FFS-LCD applications. It has been well established that a high residual DC voltage value might result in an image sticking for the LCD devices [26]. Thus, the formulation and structural characteristics of PI-8 should be modified to reduce the RDC values as low as possible. As we know, as compared to the pre-imidized PI alignment agents, their precursors, poly(amic acid)s usually exhibited much lower RDC levels [27]. Thus, it might be a compromised procedure to combine the imidized PI-8 and its PAA solution so as to achieve a balance of high VHR and low RDC levels for the TFT-LCDs. The detailed investigations are being performed in our laboratory.

| LC cells mode | Cell gap (μm) | Pretilt angle (°)* | VHR (%, 30 °C) | RDC (mV, 30 °C) |
|---|---|---|---|---|
| FFS | 5.6 | 2.7 | 98.2 | 230 |

* Measured with LC cells with 50 μm spacers.

**Table 5.** Electrical characterization of FFS-LCD cells

## 4. Conclusions

As one of our continuous endeavors developing low-cost and high performance PI alignment layers for TFT-LCDs, a systematic experiment was performed from monomer design and synthesis, PI preparation and characterization to final devices fabrication. First, several novel semi-alicyclic dianhydrides containing substituted-tetralin moiety were synthesized via a low-cost route with good yields. Then, a series of PIs were prepared from the dianhydrides and aromatic diamines. The asymmetrical alicyclic structures in the dianhydride units destroyed the regularity of the PI molecule chains; thus enhances their solubility in common solvents. Meanwhile, this irregular packing of the PI chains is beneficial for the penetration of UV and visible light. Thus, a good optical transparency is achieved in the present PIs. Incorporation of the bulky alicyclic tetralin moiety in the dianhydride units did not deteriorate their thermal stability. More importantly, the current PIs showed good orientating ability to LC molecules. The LC cells with PI-8 as the alignment layer exhibited good optoelectrical properties.

Thus, the present semi-alicyclic PIs are considered to be promising alignment layers for TFT-LCDs. Research on the applications of the PIs in large area TFT-LCD monitors are in progress now.

## Acknowledgements

Financial support from the National Natural Science Foundation of China (51173188 and 50403025) is gratefully acknowledged.

## Author details

Jin-gang Liu*, Yuan-zheng Guo, Hai-xia Yang and Shi-yong Yang

*Address all correspondence to: liujg@iccas.ac.cn

Laboratory of Advanced Polymer Materials, Institute of Chemistry, Chinese Academy of Sciences, Beijing 100190, People's Republic of China

## References

[1] Van Aerle, N.A.J.M., & Tol, A. J. W. (1994). Molecular orientation in rubbed polyimide alignment layers used for liquid-crystal displays. *Macromolecules*, 27(22), 6520-6526.

[2] Nishikawa, M. (2000). Design of polyimides for liquid crystal alignment films. *Polym Adv Technol.*, 11, 404-412.

[3] Seo, D.S., Araya, K., Yoshida, N., Nishikawa, M., Yabe, Y., & Kobayashi, S. Effect of the polymer tilt angle for generation of pretilt angle in nematic liquid crystal on rubbed polyimide surfaces. Jpn. J. Appl. Phys. (1995). LL506., 503.

[4] Nishikawa, M., Yokoyama, Y., Bessho, N., Seo, D. S., & Iimura Kobayashi, S. (1994). Synthesis of a novel organic-solvent-soluble polyimide and its application to alignment film for liquid crystal displays. *Jpn. J. Appl. Phys.*, L810-L812.

[5] Nishikawa, M., Suganuma, T., Tsuda, Y., Bessho, N., Iimura, Y., & Kobayashi, S. (1994). Properties of voltage holding ratios of liquid crystal cells using organic-solvent-soluble polyimide alignment films. *Jpn. J. Appl. Phys.*, L1113-L1116.

[6] Nishikawa, M., Sano, K., Miyamoto, T., Yokoyama, Y., Bessho, N., Seo, D. S., Iimura, Y., & Kobayashi, S. (1994). Pretilt Angles of Liquid Crystal on Organic-Solvent-Soluble Polyimide Alignment Films. *Jpn. J. Appl. Phys.*, 33, 4152-4153.

[7] Seo, D. S., Nishikawa, M., & Kobayashi, S. (1997). Generation of high pretilt angles of nematic liquid crystal (5CB) on rubbed organic solvent soluble polyimide surfaces with helical backbone structure and trifluoromethyl moieties. *Liquid Crystals*, 22, 515-517.

[8] Zhang, B. L., Li, K. K., Chigrinov, V. G., Kwok, H. S., & Huang, H. C. (2005). Application of photoalignment technology to liquid-crystal-on-silicon microdisplays. *Jpn. J. Appl. Phys.*, 44, 3983-3991.

[9] Lai, M. C., Chu, W. C., Chang, C. W., & Tsai, M. R. (2011). Liquid crystal alignment solution. 7914863, 2011-5-29.

[10] Liu, J. G., He, M. H., Zhou, H. W., Qian, Z. G., Wang, F. S., & Yang, S. Y. (2002). Organosoluble and transparent polyimides derived from alicyclic dianhydride and aromatic diamines. *J Polym Sci, Part A: Polym Chem.*, 40, 110-119.

[11] Zhang, W., Xu, H. J., Yin, J., Guo, X. X., Ye, Y. F., Fang, J. H., Sui, Y., Zhu, Z. K., & Wang, Z. G. (2001). Preparation and properties of organosoluble, colorless, and high-pretilt-angle polyimides based on an alicyclic dianhydride and long-main-chain alkyl-group-containing diamines. *J Appl Polym Sci.*, 81, 2814-2820.

[12] Nishikawa, M. (2011). Development of novel polyimide alignment films for liquid crystal display televisions. *J. Photopolym Sci Technol.*, 24, 317-320.

[13] Fairfield, G. M. S., & Norwalk, J. C. P. Preparation of dianhydrides from maleic anhydride and a vinyl benzene. 3769304, 1973.

[14] Lee, Y. J., Kim, Y. W., Ha, J. D., Oh, J. M., & Yi, M. H. (2007). Synthesis and characterization of novel polyimides with 1-octadecyl side chains for liquid crystal alignment layers. *Polym Adv Technol.*, 18, 226-234.

[15] Tsuda, Y. (2009). Soluble polyimides based on aromatic diamines bearing long-chain alkyl groups. *Mittal K L. (ed.) Polyimide and other high-temperature polymers: synthesis, characterization and applications, Koninklijke Brill, Leiden*, 5, 17-42.

[16] Wang, D. H., Shen, Z. H., Guo, M. M., Cheng, S. Z. D., & Harris, F. W. (2007). Synthesis and properties of polyimides containing multiple alkyl side chains. *Macromolecules*.

[17] Hasegawa, M., & Horie, K. (2001). Photophysics, photochemistry, and optical properties of polyimides. *Prog Polym Sci.*, 26, 259-335.

[18] Ando, S., Matsuura, T., & Sasaki, S. (1997). Coloration of aromatic polyimides and electronic properties of their source materials. *Polym J.*, 29, 69-76.

[19] Liaw, D. J., Wang, K. L., Huang, Y. C., Lee, K. R., Lai, J. Y., & Ha, C. S. (2012). Advanced polyimide materials: syntheses, physical properties and applications. *Prog Polym Sci.*, 37, 907-974.

[20] Matsumoto, T., & Kurosaki, T. (1996). Soluble and colorless polyimides with polyalicyclic structures. *React Fun Polym.*, 30, 55-59.

[21] Choi, I. H., & Chang, J. H. Colorless polyimide nanocomposite films containing hexafluoroisopropylidene group. Polym Adv Technol.. (2011). , 22, 682-689.

[22] Jang, W. B., Shin, D. Y., Choi, S. H., Park, S. G., & Han, H. S. (2007). Effects of internal linkage groups of fluorinated diamine on the optical and dielectric properties of polyimide thin films. *Polymer*, 48, 2130-2143.

[23] Lee, S. H., Hong, A. H., Kim, J. M., & Lee, J. Y. (2001). An overview of product issues in wide-viewing TFT-LCDs. *J SID.*, 155-160.

[24] Lyu, J. J., Sohn, J. W., Kim, H. Y., & Lee, S. H. (2007). Recent trends on patterned vertical alignment (PVA) and fringe-field switching (FFS) liquid crystal displays for liquid crystal television applications. *J Display Technol.*, 3, 404-412.

[25] Huang, J. Y., Li, J. S., Juang, Y. S., & Chen, S. H. (1995). Rubbing-induced molecular alignment on an orienting layer of polyimide with and without alkyl side chains. *Jpn. J. Appl. Phys.*, 34, 3163-3169.

[26] Masanobu, M., Tetsuya, M., & Tatsuo, U. (2011). Interaction between Impurity Ions and Alignment Polymer Layers Affecting the Image Sticking Effect on Liquid Crystal Displays. *Kobunshi Ronbunshu in Japanese*.

[27] Seen, S. M., Kim, M. S., & Lee, S. H. (2010). Image sticking resistant liquid crystal display driven by fringe electric field for mobile applications. *Jpn J Appl Phys.*